Extraction of Quantitative Meteorological Information from INSAT Imagery

By R.R. Kelkar and A.V.R.K. Rao

Division of Satellite Meteorology, India Meteorological Department, New Delhi-110 003
(Manuscript received 14 May 1991, in revised form 25 August 1991)

Abstract

The paper presents a review of techniques being used for the retrieval of quantitative meteorological information from INSAT VHRR (Very High Resolution Radiometer) data. It describes how the constraints imposed by the spacecraft design and the ground segment capabilities led to the development of innovative and unconventional techniques of product retrievals from INSAT.

The utility of the INSAT derived products, viz. Cloud Motion Vectors, Sea Surface Temperature, Outgoing Longwave Radiation and Quantitative Precipitation Estimates is discussed. The variation of these parameters on different space and time scales is presented.

1. Introduction

Indian meteorologists began using meteorological satellite data operationally in 1965 when the first APT reception station was established at Bombay. By 1980, India had a network of eight APT stations providing images received from polar-orbiting satellites to operational forecasters. The images could not be processed further as no digital data was available. Moreover, their resolution was low, aerial coverage was limited to India and the neighborhood and the orbiting satellites re-visited an area only after 12 hours. The use of satellite data in the sixties and seventies, therefore, remained confined to a visual interpretation of APT images and drawing qualitative inferences from the brightness, size or configurations of clouds as seen in them.

Satellite Meteorology in India may be said to have really come of age in 1982 with the advent of India's own multi-purpose geostationary satellite system having radiometric imaging and data relay capabilities. The first satellite of the series INSAT-IA, had unfortunately a short life. However, its successor spacecraft, INSAT-IB provided over 30,000 image scans of the earth between October 1983 and July 1990 when its functions were taken over by INSAT-ID, the last satellite of the INSAT-I series.

To process the data from the VHRR (Very High Resolution Radiometer) and DRT (Data Relay Transponder) on-board the INSAT Satellite, the India Meteorological Department established in 1982 a Meteorological Data Utilization Centre (MDUC) at New Delhi. The MDUC computer system was integrated around a set of two PDP 11/34 and two PDP 11/70 computers for processing the VHRR stream and another two PDP 11/34 computers for the DCP (Data Collection Platform) data received through the DRT. The system architecture was basically designed to meet the requirements of (i) real-time processing of INSAT digital data, (ii) making it available to image analysts through hard copies and on interactive displays, (iii) disseminating the images to remote locations and (iv) archival of the data on computer compatible tapes.

While the primary functions of MDUC continued to be carried on, a considerable amount of software development effort was made in the middle and late eighties, to fully exploit the system capabilities for derivation of quantitative meteorological products from the digital INSAT VHRR data. It was not only the limited system resources that posed a challenge to the development work but the design of the INSAT satellite itself which had many basic differences from other meteorological satellites. These two factors led to the innovation of techniques of quantitative product derivation, which could be termed in a sense, un-conventional. For example, MDUC attempted, with success, the derivation of Cloud Motion Vectors from INSAT visible images (because of its good resolution of 2.75 km in visible and the low resolution of 11 km in the infra-red). Whereas NOAA makes only twice-daily OLR (Outgoing Longwave Radiation) measurements with the orbiting satellites, use of 3-hourly images make the INSAT OLR values more authentic. Again, although INSAT has a single 10.5–12.5 μ infra-red window with 11 km resolution, it is being used to

retrieve the sea surface temperature, in spite of this limitation by using a specially developed technique. While INSAT precipitation estimation follows in most respects methodologies used internationally, the study of monsoon behavior has been attempted through an analysis of the fractional clouding itself.

This paper reviews the various techniques which have been developed for quantitative product generation from INSAT data and discusses some of the latest results, obtained particularly with Cloud Motion Vectors, Sea Surface Temperature, Outgoing Longwave Radiation and Quantitative Precipitation Estimates.

2. Cloud motion vectors

Despite their inherent errors and uncertainties, satellite-derived Cloud Motion Vectors (CMVs) are very useful as they constitute virtually the only source of upper wind data over the vast oceanic areas of the glove. Around the Indian Peninsula in particular, the only radiowind stations are those located on the Lakshadweep Islands in the Arabian Sea and in the Andaman Islands in the Bay of Bengal. CMVs therefore appear to be the best means of augmenting the conventional data in the day-to-day synoptic analysis of flow patterns over the Indian Ocean.

Extraction of CMVs from INSAT-IB images was made operational in November 1984 and the procedures have since undergone several stages of improvement and refinement (Kelkar *et al.*, 1986, 1987 and Yadav and Kelkar, 1989). Since the resolution of the INSAT-1 VHRR is 2.75 km in the visible channel and 11 km in the infra-red channel, the visible INSAT images are used for the cloud tracking. The procedure requires three full-resolution, sectorised, navigated and registered images, two of which are visible images for time T and T+30 minutes and the third is an i-r image for time T. The CMVs are derived daily with the 0300 and 0330 UTC pair of INSAT images and the 0600 and 0630 UTC pair of images. The 0600 UTC CMVs are disseminated over the WMO Global Telecommunication system, while the 0300 UTC CMVs are used nationally. Illumination considerations do not permit CMV extraction at the standard synoptic hours of 0000 and 1200 UTC, since the cloud tracking is done on the basis of visible imagery.

2.1 Methodology

The INSAT CMV extraction is attempted at 225 locations (15×15 matrix) within an image sector approximately 14°×14°lat/long in extent. Six such sectors are in use and they cover the Arabian Sea, Bay of Bengal, and western parts of the Indian Ocean (Fig. 1). Around each of the 225 locations in a sector, a reference window of 15×15 pixels in

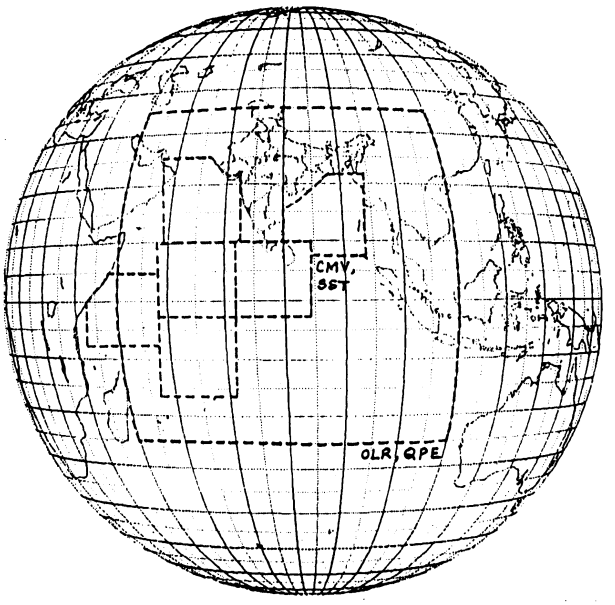

Fig. 1. INSAT-1D image sectors over which quantitative products are derived.

the visible image of time T is taken. An operator-specified grey scale threshold is applied to all points of the reference window and CMV extraction is not attempted if it consists of large cloud patches or clear skies. The search window from the image of time T+30 minutes has the same centre as that of the reference window but its size is 37×37 pixels for low clouds or 61×61 pixels in the case of medium and high clouds.

The automated pattern matching technique computes the absolute difference of grey shade between corresponding pixels of the reference window (a_n) and a subset of the search window (b_n) of the same size as the reference window. These differences are summed up to arrive at a mean value for each subset i of the search window.

$$\overline{Xi} = \frac{\sum_{i=1}^{225} |a_n - b_n|}{225}$$

The centre of the particular subset in which $\overline{Xi}$ is the minimum, is taken as the end-point B of the cloud motion vector, its origin A being the centre of the reference window.

The wind speed and direction are obtained from the relative pixel shifts (north-south and east-west) between points B and A in 30 minutes, and the wind is located at point A. For assigning the heights to the CMV, the sea surface temperature is required to be input and a standard lapse rate of 6.5°C/km is thereafter applied. The height is interpolated from the mode of the cloud top temperature in the portion of the infra-red image corresponding to the reference window in the visible image.

After the CMVs of one complete sector are extracted by the automated process, they are interactively displayed for low (<3 km), medium (3–8 km) and high (>8 km) levels separately for visual examination along with the underlying visible and infrared images. At this stage, the analyst applies three different criteria as follows to eliminate spurious vectors from the data set:

(a) Gradient check: Any abrupt change in the direction or speed within a cluster of CMVs, when there is likelihood of a simple uni-directional flow, is not accepted. However, there could be particular situations wherein strengthening or weakening of winds and veering/backing of winds may appear to be realistic.

(b) Inter-comparison check: The INSAT CMVs are examined in relation to other observations such as radiowind/pilot balloon data from coastal and island stations, wherever available.

(c) Synoptic check: Those CMVs which are not supporting the synoptic features over the area, and those which are not in consonance with the cloud configuration are rejected. However, if meso-scale phenomena are required to be retained, this check has to be applied judiciously.

Spurious CMVs get eliminated in the above quality control process and result in the generation of a cohesive data set which is then ready for dissemination.

2.2 Applications

Besides their use in daily synoptic analysis and forecasting, INSAT CMVs provide a wealth of information over the Indian Ocean region not hitherto available, particularly in relation to the Indian summer monsoon. The CMVs have proved to be useful for studying the formation of eddies, the cross-equatorial flow, the approach of the southwest monsoon towards the west coast of India, the offshore vortices and the activity of the two separate branches of the monsoon as in a case study of the 1987 monsoon (Yadav and Kelkar, 1989).

Previous studies of Indian Ocean winds were made either as a part of specially organized experiments such as IIOE in 1964–65 and MONEX in 1979 during which the GOES satellite was temporarily parked over the Indian Ocean. Now, using INSAT CMVs, Sant Prasad *et al.* (1990) have constructed mean monthly wind fields over the Indian Ocean for the period April–July 1988. They have been able to relate these patterns to the changes in the atmospheric flow from the pre-monsoon to monsoon conditions. They have also computed the mean monthly vergence and vorticity patterns for this period. Figures 2 and 3 show the low-level and high-level wind patterns respectively for the four months of April-July 1988, which was a very good monsoon year. The April low-level pattern is characterized by a ridge line running across 15°N. In June, the cross-equatorial flow is clearly seen and both the branches of the monsoon appear to be well-established. The winds in the Bay of Bengal converge towards the Head Bay. The July pattern brings out the monsoon trough.

In the higher levels, the ridge line in April lies along 10°N in the northern hemisphere and 10°S in the southern hemisphere. The June and July fields bring out the easterly flow which is characteristic of the monsoon.

A typical CMV chart during the onset phase of the southwest monsoon (30 May 1990) is shown in Fig. 4. This chart depicts the low-level flow a day prior to the onset of the monsoon over Kerala. Strong winds of the order of 20–30 knots off the Somali Coast are indicative of the development of the low-level jet.

3. Sea surface temperatures

Compared with the complexities of other satellite retrievals, the physics of sea surface temperature extraction over cloud-free areas is much simpler. However, a major practical difficulty arises from the fact that the 10.5–12.5 μ infra-red window, used commonly in radiometers of meteorological satellites is not perfectly transparent to the emission from the sea surface. The result is that the satellite brightness temperature of the sea surface is always lower than the actual SST. In the early years of satellite meteorology, many workers attempted to parameterize the attenuation effect to enable a correction to be applied to the brightness temperature to obtain the SST. However, after 1981, with the introduction of the split-window radiometer channels on the NOAA satellites, the multi-channel algorithms came into vogue for retrieval of SST by simply eliminating the atmospheric effects.

The INSAT series of satellites have continued to have a single 10.5–12.5 μ window, necessitating the application of a correction term for the SST retrieval. The correction term has been obtained as a function of water vapour and brightness temperature by working backwards from the MCSST algorithm and using laboratory measurements of transmission function for the 10.5–11.5 and 11.5–12.5 μ wavelength bands for different water vapour amounts. Kelkar *et al.* (1989) have described the methodology in detail. Here, the radiance received by the radiometer in a single channel 10.5 to 12.5 μ, is considered to have been made up of two component radiances in the 10.5 to 11.5 and 11.5 to 12.5 μ windows. The partitioning of the radiance depends upon the atmospheric water vapour which if known, allows one to simulate the two window radiances and hence the corresponding window brightness temperatures. From these temperatures, the SST value can be derived through an application of the MCSST algorithm. It is not necessary to use the procedure

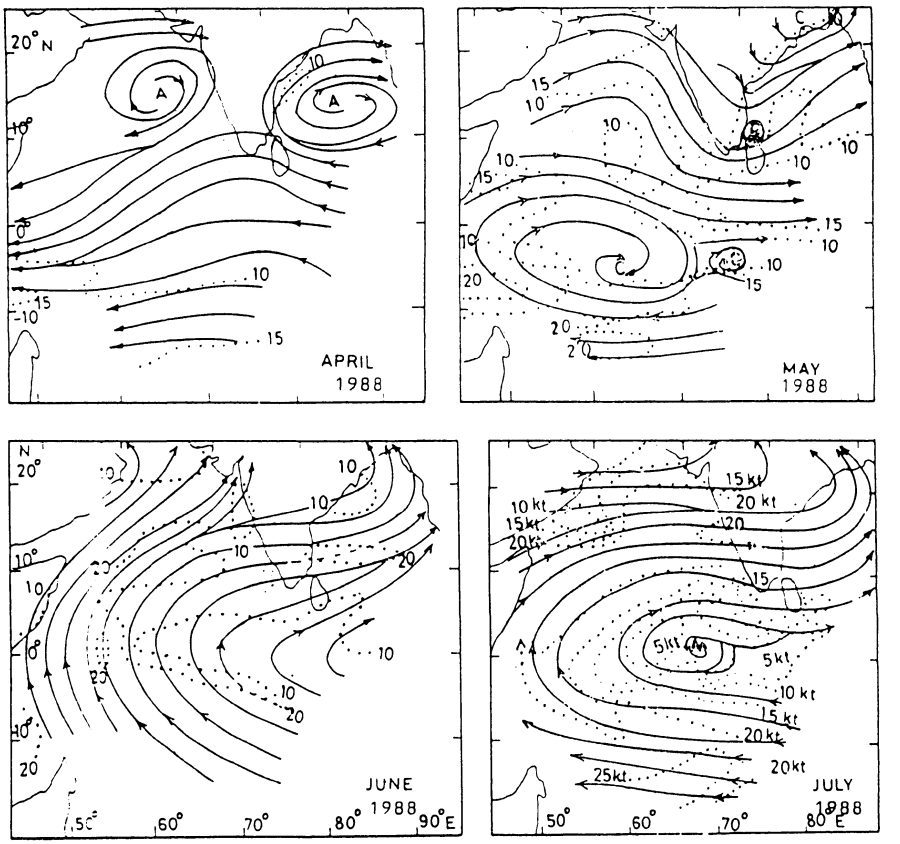

Fig. 2. Mean monthly upper wind patterns derived from daily 0600 UTC low-level Cloud Motion Vectors. (Dotted lines are isotachs in knots)

each time, but a family of curves for various values of single window brightness temperature and the atmospheric water vapour content is constructed once and then used for interpolation. Routine derivation of SST from INSAT data commenced in Sept. 1985 for three oceanic sectors around India, covering the Bay of Bengal, Arabian Sea and the Indian Ocean north of 3S latitude, at 0300 and 0600 UTC daily.

The software used for the SST retrieval divides each sector into 225 (15×15) boxes and the warmest brightness temperature amongst the pixels in the box is chosen. Boxes having brightness temperature less than 280°K or more than 300°K are not considered for further processing to minimize cloud or land contamination. The atmospheric water vapour required for computing the correction term is taken from climatological data. Since the viewing angle of the satellite radiometer increases with distance from the sub-satellite point, the increased attenuation along the slant path has to be computed from geometric considerations. After the corrected SSTs are obtained, the software applies a gradient check to the SST field to reject SSTs which are different from their neighbors by more than a specified value. Kelkar *et al.* (1989) made a comparison of INSAT SSTs with colocated NOAA SSTs and found that out of the total population of colocated samples studied, 50% agreed within ±1°C and 75% were within ±2°C.

It has been the experience that during the monsoon months, very few SST retrievals are possible because of extensive clouding in the region but in other months SST retrievals with sufficient detail are possible. Typical SST analysis for a clear day in the pre-monsoon season is given in Fig. 5.

4. Outgoing longwave radiation

The outgoing flux of longwave radiation from the earth-atmosphere system is an important component of the overall planetary radiation budget. What the satellites measure, on the other hand, is the radiance received in a very narrow window in the infra-red region of the spectrum, and these measurements cannot be directly utilized in radiation budget studied on a planetary scale. It is, however, possible to extrapolate the outgoing longwave radiation (OLR) from the satellite brightness temperature through a regression equation of the form:

$$T_f = T_b\,(a + b \cdot T_b)$$

where T_b is the brightness temperature, T_f is the so-called flux temperature, both in °K, and a, b are regression constants. OLR is then computed

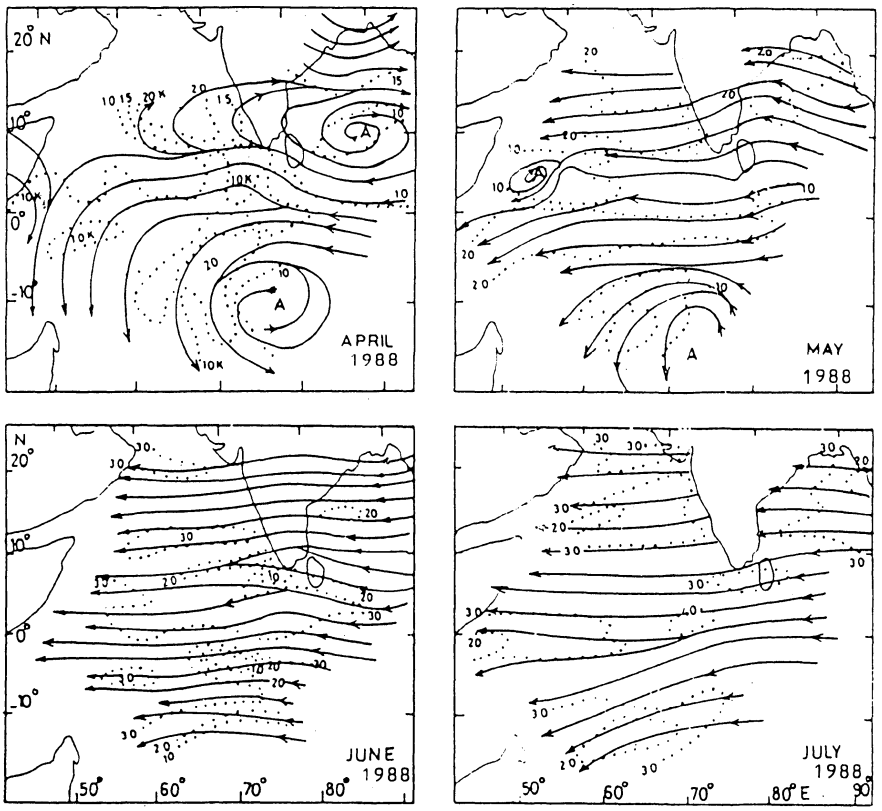

Fig. 3. Mean monthly upper wind patterns derived from daily 0600 UTC high-level Cloud Motion Vectors. (Dotted lines are isotachs in knots)

as σT_f^4, where σ is the Stefan-Boltzmann constant. In the case of the INSAT 10.5–12.5 μ channel, the constants a and b have values of 1.1889 and 0.000989/°K respectively, both decreasing as the zenith angle increases (Rao *et al.*, 1989, Arkin *et al.*, 1989).

Regular OLR computations from INSAT data were started in June 1986. The computations are performed over 2.5×2.5°lat/long boxes within the area 40°–100°E, 35°N–25°S with 3-hourly images. (The longitudinal coverage is presently 50–110°E with INSAT-ID). The mean brightness temperature for a box is first derived and then the regression equation is applied to get the OLR, using the appropriate zenith angle. It has been found that the OLR derived from the mean temperature does not vary appreciably from the value which would be obtained if OLRs were derived for each pixel in a box and then averaged. This also leads to a significant saving of processing time.

4.1 OLR seasonal variations

From the 3-hourly values of OLR, daily, weekly and monthly averages are produced. The mean monthly maps of OLR for the period June 1986 to December 1988 have been published (IMD, 1988, 1990). Monthly OLR maps for the monsoon season of 1986 have been discussed by Arkin *et al.* (1989) and those for the winter months of 1986-87 have been studied by Rao *et al.* (1989). It has been found that the INSAT OLR correlates very well with NOAA OLR, with pattern correlation coefficients exceeding 0.95, although there is a suggestion of a positive bias of 5–10 watts/m^2 in the NOAA values over land compared to INSAT values. The INSAT OLR daily values are built up from eight observations per day as against two used by NOAA, which could be one of the reasons for the difference. INSAT OLR therefore provides additional detailed information which cannot be obtained from polar-orbiting satellite derivations.

In general, the monthly OLR means in winter (Fig. 6–Jan 1989) are characterized by a predominantly zonal orientation of isopleths. The lowest values (<180 watts/m^2) are observed over the Tibetan Plateau while the highest values (>260 watts/m^2) are found along 15°–20°N latitudes. In the southern hemisphere, which is experiencing summer at the time, OLR values are again low (<240 watts/m^2) corresponding with increased convective activity.

In the monsoon season (Fig. 6–July 1989) the highest values (>280 watts/m^2) are seen over the north-western sector comprising the Arabian peninsula and Iran. Over Arabian Sea the OLR isopleths are oriented in a north-south direction with values decreasing eastwards rapidly to a minimum (<200

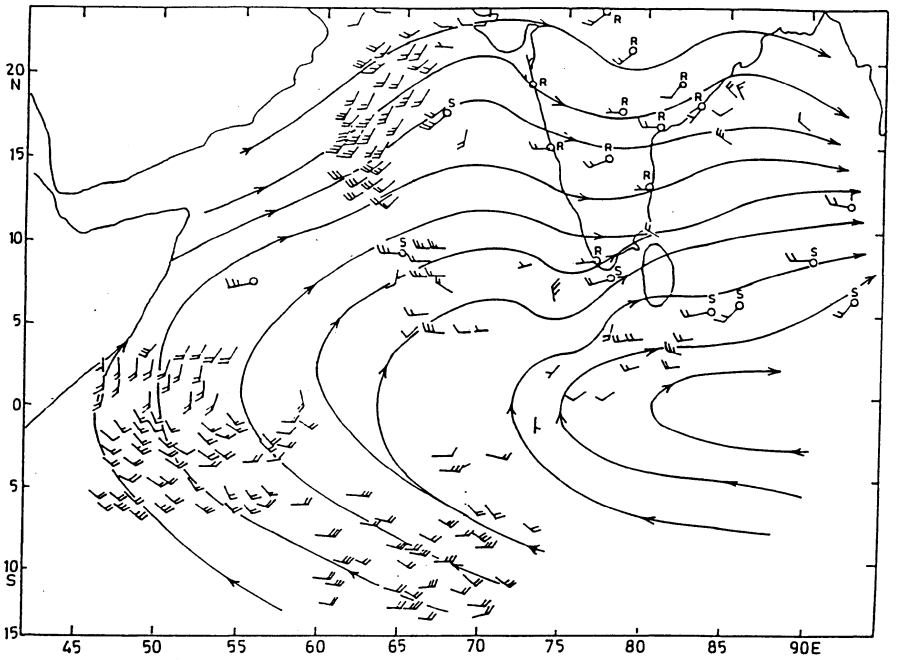

Fig. 4. 0600 UTC low-level Cloud Motion Vectors for May 30, 1990 (Onset phase of south-west monsoon).

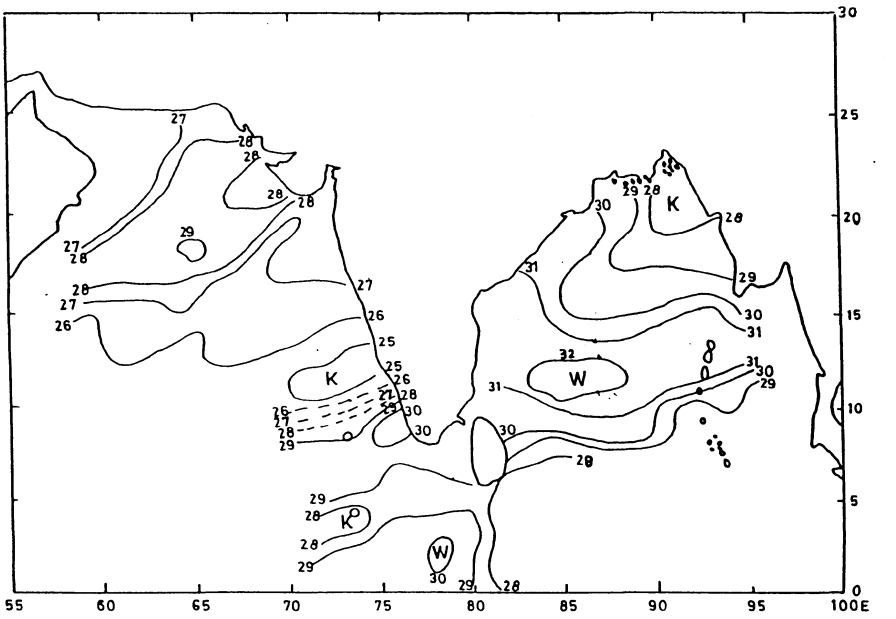

Fig. 5. INSAT Sea Surface Temperatures over the oceanic regions around the Indian peninsula for 25 April 1990, 0600 UTC.

watts/m^2) over central and eastern India. Over the 0–10°S belt of the southern hemisphere the OLR values are mostly of the order of 220 watts/m^2.

Rao *et al.* (1989) have confirmed from the monthly mean OLR maps that OLR is a good index of convective activity and is inversely related to the precipitation amounts. They have found that 250 watts/m^2 is a threshold which demarcates raining and non-raining areas while the 240 watts/m^2 isopleth delineates the area of appreciable rainfall on a monthly scale.

4.2 Diurnal variation of OLR

Since INSAT is a geostationary satellite, more frequent computation of OLR during the diurnal cycle is possible than with the polar-orbiting NOAA satellites which produce twice-daily values. This helps to study the diurnal variation in greater detail and

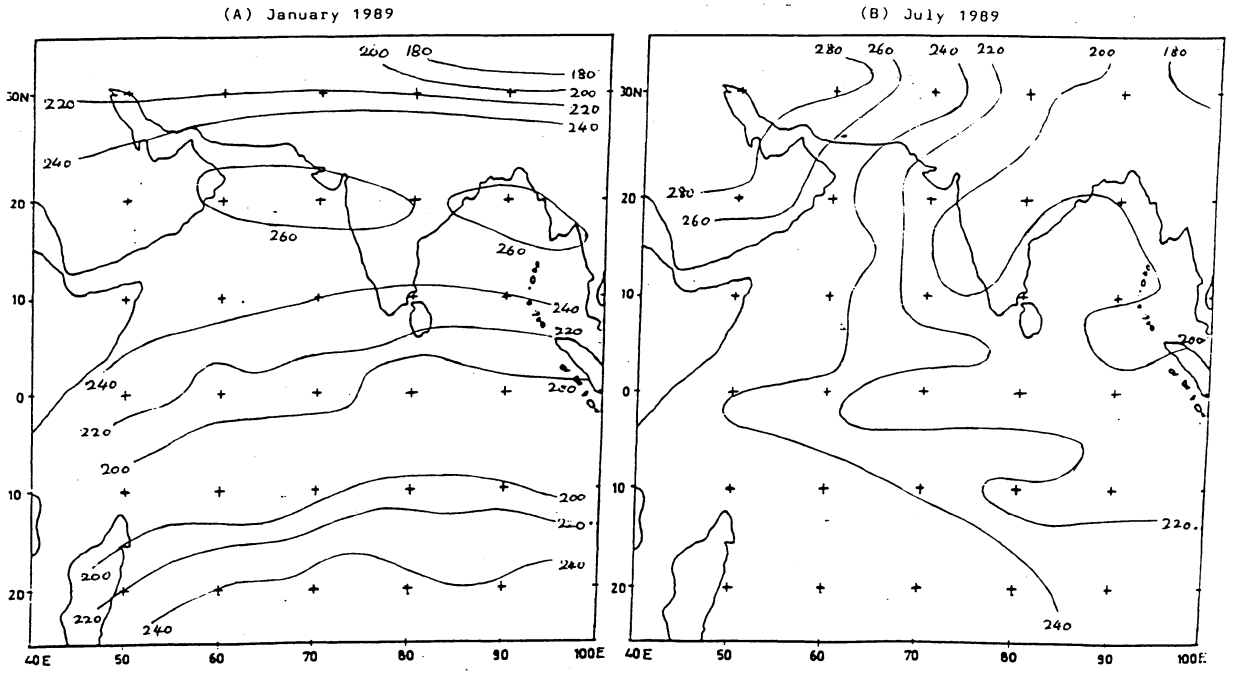

Fig. 6. Mean monthly INSAT Outgoing Longwave Radiation (watts/m^2) for January and July 1989.

yields a more accurate daily average. Figures 7a to 7d show the variety of the diurnal regimes of OLR as computed from INSAT data over different surfaces in different seasonal situations. The OLR values plotted in the figures are means of monthly values for three years 1987, 1988 and 1989.

Figure 7a represents the desert region of Rajasthan over northwest India (27.5N, 72.5E), where the highest values of the order of 300–320 watts/m^2 are seen in the clear months of April and October at 0600–0900 UTC corresponding to about 1100–1400 local time. Minimum values of 200 watts/m^2 occur at 2100–0000 UTC *i.e.* 0200–0500 local time, with a high diurnal range of 70 watts/m^2 in April. The January curve shows a very similar trend, but the OLR values vary between 220 and 280 watts/m^2 because of the low surface temperatures in winter. In the monsoon season, however, there is a distinct change and the curve is more flat, varying between 220 and 240 watts/m^2 only. The July minimum is not very distinct and spreads over 1500–2100 UTC (2000–0200 local time).

Figure 7b is typical of a monsoon regime over land (north-east India 25.0N, 85.0E). The July curve is very distinct from the curves from other months, with OLR values varying from a maximum of only around 200 watts/m^2 at 0300 to 0600 UTC (0900 to 1200 local time) to a minimum of 160 watts/m^2 at 1200 UTC (1800 local time) which is the time of maximum convective activity. In other seasons, the diurnal OLR curve appears to be modulated by the surface temperature variations, with an early morning minimum and a noon-time maximum.

The diurnal variation of OLR over the central Bay of Bengal (12.5N, 87.5E) is shown in Fig. 7c. As the SST variations are small over the day, the curves are characterized by their flatness in all the seasons as against the land patterns which exhibit large diurnal ranges. The July values are however consistently lower (200 watts/m^2) compared to the January and April values (250–260 watts/m^2), showing that the cloudiness over the Bay of Bengal persists throughout the day and night during the monsoon season.

Figure 7d is typical of the oceanic area within the SHET region (Eq., 85.0E). Here not only is the diurnal range very small, but the seasonal differences are also very low. All OLR values are confined to a narrow range of 210–240 watts/m^2 for the year as a whole.

5. Quantitative precipitation estimates

Monsoon rainfall exhibits a variability on various time scales, such as the 5–7 day synoptic scale variability, the 15-day or 30–40 day low-frequency modes, and the inter-annual or longer time-scale variability. Studies of these variabilities require areally averaged rainfall to be known. Large-scale precipitation values are also of importance in many fields like hydrology, agriculture, climatology and numerical modelling. However, estimation of areal rainfall from point measurements by raingauges is known to be subject to many types of errors. Further, rainfall data over the vast oceanic areas and other inaccessible terrain are almost absent. In these respects, satellite-based estimates of rainfall are of great value.

Quantitative Precipitation Estimates (QPE) are being made from INSAT infra-red data regularly

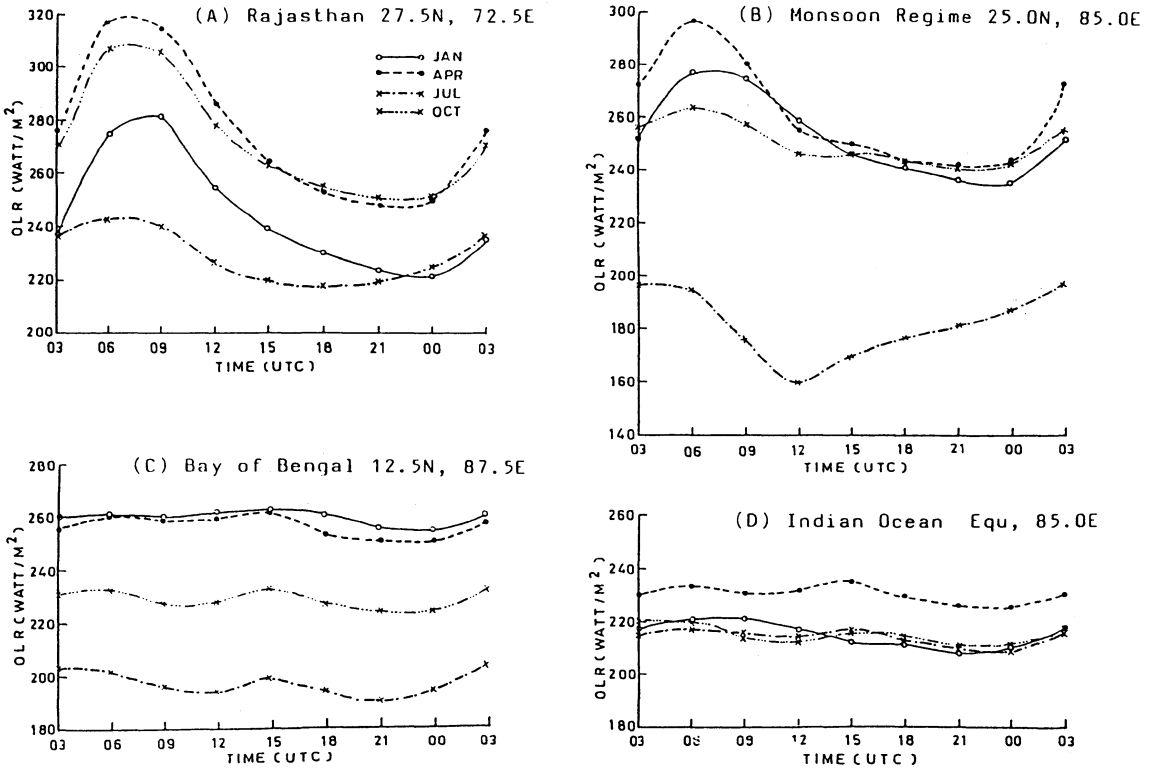

Fig. 7. Typical patterns of diurnal variation of INSAT Outgoing Longwave Radiation (Monthly average for 1987–89).

since June 1986. The methodology which is described in detail by Rao *et al.* (1989) and Arkin *et al.* (1989) is based upon the use of full-resolution i-r data at 3-hourly interval. The area over which QPE is derived extends from 35N–25S and 40–100E (50–110E for INSAT-ID) and it is further sub-divided into 2.5×2.5°lat/long boxes. The ratio of cloudy pixels colder than 235K in a box to the total number of pixels in it is computed for each box. By using 3-hourly data, such ratios of fractional clouding are computed for daily, weekly and monthly time scales. The precipitation is then obtained as the product of the fractional clouding, the number of days over which the accumulation of data is done and a constant 71.2 mm/day which is the assumed rain rate.

5.1 Mean QPE patterns

The mean precipitation patterns for the four monsoon months of June, July, August and September derived from QPE data for three years 1986–88, are shown in Fig. 8. These have been presented and discussed in detail by Kelkar *et al.* (1990). Out of the three years, 1986 was a near-normal monsoon year, 1987 was marked by unprecedented deficit rainfall, while 1988 was a very good monsoon year. The mean for the three years, therefore, covers an extreme range of values.

In the month of June, two maxima of rainfall are evident north of the equator over the eastern Arabian Sea (500 mm) and north Bay of Bengal (700 mm), with a minimum (100 mm) located in between over Sri Lanka. In July, the rain area extends further north-westwards to cover almost the whole of India, in conformity with the progress of the monsoon. The Arabian Sea maximum disappears while the Bay of Bengal maximum is less intense and moves southwards.

The August pattern is not very different except for the intensification of the maximum over the south-eastern Indian Ocean. In September, the retreat of the southwest monsoon from the Indian mainland is reflected well, while the southern hemispheric maximum continues to build up over the ocean off Sumatra Islands. Western Arabian Sea has very little rain except in June.

5.2 Validation of INSAT precipitation estimates

Arkin, Rao and Kelkar (1989) compared the weekly QPE values for the monsoon season of June–September 1986 with weekly raingauge totals for 34 meteorological sub-divisions of India. Linear regression analysis was performed and correlation coefficients were obtained for QPE derived not only with 235°K threshold, but also with other thresholds between 190 and 270°K. For 235°K, high correlations (>0.79) were found (Fig. 9) in 12 sub-divisions, and good correlations (>0.69) in 19 sub-divisions.

Lower correlations were observed over the entire west coast and parts of north-east and north-west India. The slopes of the regression slopes were

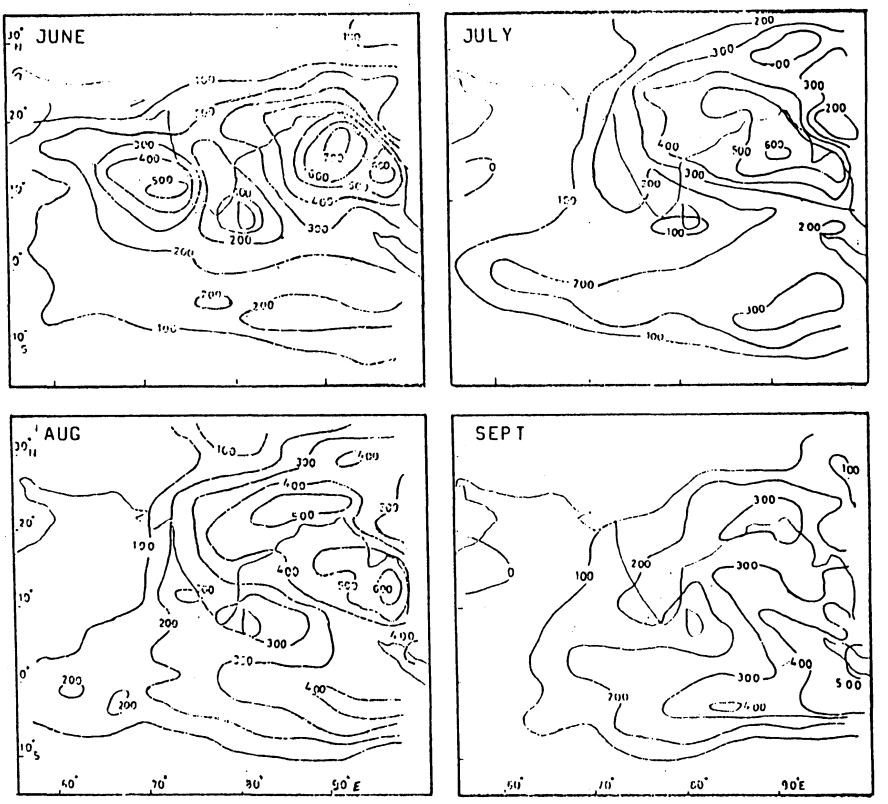

Fig. 8. INSAT-derived precipitation in mm/month (average for 1986–88) during the four months of the monsoon season.

slightly less than unity in those sub-divisions where the correlations were high, indicating that QPEs were overestimated by 10 to 20 per cent compared to raingauge totals. In a few sub-divisions, particularly the hilly areas of north and east India, and the Western Ghats the regression slopes were greater than unity suggesting an underestimate in QPE. Change of threshold values from 235° to 265°K led to significant improvement in correlations over Northwest India and west coast but three sub-divisions had low correlations regardless of the threshold tried.

This analysis confirms that the QPE algorithm can be used over land by judiciously modifying the rain rate constant of 71.2 mm/day which was originally developed by Arkin for application to oceanic regions of the Atlantic.

5.3 Use of fractional clouding

Although the fractional clouding can be related to the convective rainfall over large scales of space or time, it has been found that the fractional clouding, per se, can be used for the study of the intraseasonal modes of the monsoon. Using a threshold of 260°K (representing most of the convective clouds with tops above 8 km), Rao *et al.* (1990) analyzed time-latitude sections of fractional clouding over the southwest monsoon regime for two years 1986 and 1987. They observed that the cloud maxima had a regular northward movement starting from the

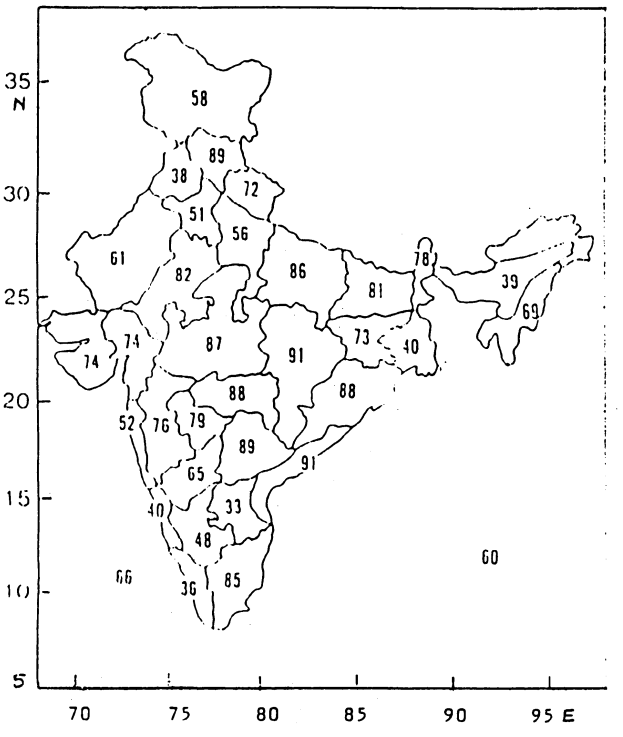

Fig. 9. Correlation (×100) between weekly QPE and areally averaged rainfall over the meteorological sub-divisions of India in the 1986 monsoon season.

equatorial Indian Ocean to about 30°N latitude with a periodicity of 30–40 days. The phase speed is about 0.9°Lat/day. Rao *et al.* also subjected the data to a spectral analysis for 5° latitude zones of 10° longitude in width. The mode gets obliterated by 25°N. In the bad monsoon year of 1987, the periodicity was enhanced in 20–25°N latitude belt. Rao *et al.* also studied the westward movement of transient disturbances on the basis of the fractional clouding and found that in 1987, the transient activity was relatively suppressed.

6. Conclusion

The paper has presented a review of techniques in vogue for retrieval of quantitative meteorological information from INSAT data. The products have been found to be very useful not only in day-to-day weather analysis but also sufficient data have now been accumulated to construct mean monthly maps of various parameters over the Indian Ocean which has so far been a data-sparse area. Some of the data have already been published and the Cloud Motion Vectors are being disseminated daily over the GTS.

The limitations of the techniques described here which are not related to satellite design constraints, will be overcome shortly when more computer processing power becomes available. The MDUC computer system is being upgraded and modernized by end of 1991 after which it will become possible to employ more sophisticated retrievals algorithms, to enlarge the area of product retrievals and improve the speed of computation and dissemination of products. The successor satellite series INSAT-II, the first of which is scheduled for launch in January 1992, will have a VHRR with an improved resolution of 2 km in the visible and 8 km in infra-red. This will make it possible to have a better use of the infra-red channel than with INSAT-I.

References

Arkin P.A., Rao A.V.R.K. and Kelkar R.R., 1989: "Large-Scale Precipitation and Outgoing Longwave Radiation from INSAT-IB during the 1986 Southwest Monsoon Season", *J. Climate*, **2**, 619–628.

IMD, 1990: "Satellite-Derived Monthly Mean Precipitation and Outgoing Longwave Radiation Maps over India and Neighborhood for the period June 1986 to December 1987", *Met. Monograph No. Sat. Met/No. 3/1988*, India Meteorological Department, New Delhi, 46 pp.

IMD, 1990: "Satellite-Derived Monthly Mean Precipitation and Outgoing Longwave Radiation Maps over India and Neighborhood for 1988", *Met. Monograph No. Sat. Met/No. 4/1990*, 30 pp.

Kelkar R.R. and Khanna P.N., 1986: "Automated Extraction of Cloud Motion Vectors from INSAT-IB imagery", *Mausam*, **37**, 495–500.

Kelkar R.R. and Rao A.V.R.K., 1990: "Interannual Variability of Monsoon Rainfall as Estimated from INSAT-IB data", *Mausam*, **41**, 183–188.

Kelkar R.R., Sant Prasad and Mani Gandeswaran S., 1987: "Spatial and Temporal Homogeneity in a Half-Hourly Sequence of Satellite-Derived Upper Winds", *Mausam*, **38**, 197–202.

Kelkar R.R., Tiwari V.S. and Sant Prasad, 1989: "Retrieval of Sea Surface Temperature from INSAT-IB radiometer Measurements using a Multi-Channel Simulation Approach, *Mausam*, **40**, 13–18.

Rao A.V.R.K., Kelkar R.R. and Arkin P.A., 1989: "Estimation of Precipitation and Outgoing Longwave Radiation from INSAT-IB Radiance Data", *Mausam*, **40**, 123–130.

Rao A.V.R.K., Bohra A.K. and Rajeswara Rao V., 1990: "On the 30–40 day Oscillations in Southwest Monsoon: A Satellite Study", *Mausam*, **41**, 51–58.

Sant Prasad, Khanna P.N., Rao A.V.R.K. and Kelkar R.R., 1990: "Satellite-Derived Monthly Average Wind Fields over the Indian Ocean in April–July 1988", *Mausam*, **41**, 445–450.

Yadav B.R. and Kelkar R.R., 1989: "Lower Level Wind Flow over the Indian Ocean during the Onset of Monsoon—1987", *Mausam*, **40**, 323–328.

INSAT 画像資料からの定量的気象情報の抽出

R.R. Kelkar • A.V.R.K. Rao
(インド気象局衛星気象部)

当論文においてはINSAT VHRR（高分解能放射計）データから定量的な気象情報を取得する技法についてのレビューを行なう。衛星の設計と地上施設の能力からくる制約に対処して、INSATプロダクトの新しい取得技法が如何に開発されたかを述べる。

またINSATから取得されたプロダクトの利用例、即ち雲移動ベクトル、海面水温、外向長波放射および定量的降雨量推定について議論する。異なった時空間スケールにおけるこれらの諸量の変動についても示す。